ELASTIC PROPERTIES OF CARBON NANOTUBES AND THEIR HETEROJUNCTIONS

N.A. SAKHAROVA[*], J.M. ANTUNES[*†], A.F.G. PEREIRA[*], B.M. CHAPARRO[†] AND J.V. FERNANDES[*]

[*] CEMMPRE – Department of Mechanical Engineering, University of Coimbra,
Rua Luís Reis Santos, Pinhal de Marrocos
3030-788 Coimbra, Portugal
e-mail: {nataliya.sakharova, andre.pereira, valdemar.fernandes}@dem.uc.pt,
www.uc.pt/en/iii/research_centers/CEMUC

[†] Escola Superior de Tecnologia de Abrantes, Instituto Politécnico de Tomar
Rua 17 de Agosto de 1808-2200 Abrantes, Portugal
email: jorge.antunes@ipt.pt, bruno.chaparro@sapo.pt, http://www.esta.ipt.pt

Key words: Carbon Nanotubes, Carbon Nanotubes Heterojunctions, Elastic Properties, Numerical simulation.

Abstract. Comprehensive studies on the modelling and numerical simulation of the mechanical behaviour under tension, bending and torsion of single-walled carbon nanotubes and their heterojunctions are performed. It is proposed to deduce the mechanical properties of the carbon nanotubes heterojunctions from the knowledge of the mechanical properties of the single-walled carbon nanotubes, which are their constituent key units.

1 INTRODUCTION

Systematic research has been conducted for studying nano-materials such as carbon nanotubes (CNTs) that are efficient components for designing new materials with required electronic and mechanical properties [1] and building blocks for optical and electronic nanodevices [2]. The CNT heterojunctions (two connected CNTs) are necessary constituents for such nanodevices as circuits, amplifiers, switches and nanodiodes [3]. The understanding of the CNTs' mechanical properties is indispensable in order to design composites reinforced with CNTs and CNT-based devices, since their stability and efficiency are dependent on the mechanical properties of the constituents, i.e. CNTs and CNT heterojuctions.

The elastic properties of CNTs can be assessed using experimental techniques (atomic force microscopy (AFM) and transmission electron microscopy (TEM) [4]) and computational approach. There are three main groups of methodologies for the modelling of CNTs mechanical behaviour: the atomistic approach, the continuum mechanics approach and the nanoscale continuum mechanics approach. In case of the nanoscale continuum modelling approach (NCM) each carbon-carbon (C-C) bond is replaced by a solid element, e.g. a beam element, whose behaviour is described by elasticity theory (see, [5, 6]).

A considerable part of the theoretical investigations has been devoted to the predicting of

the Young's modulus of single-walled carbon nanotubes (SWCNTs) [5, 6]. Less attention has been paid to understanding the mechanical behaviour of nanotube heterojunctions.

The present work is focused on the characterisation of mechanical properties of SWCNTs in a wide range of chiral indices, diameters as well as SWCNT cone-heterojunctions by modelling their structure and mechanical behaviour, using nanoscale continuum approach [5].

2 ATOMIC STRUCTURE OF CNTS AND THEIR HETEROJUNCTIONS

An ideal single-walled nanotube can be seen as a rolled-up graphene sheet, whose surface is composed by the repeated periodically hexagonal [2]. The symmetry of the atomic structure of a nanotube is characterized by the chirality, which is defined by the chiral vector $\boldsymbol{C_h}$:

$$\boldsymbol{C_h} = n\boldsymbol{a_1} + m\boldsymbol{a_2} \tag{1}$$

where n and m are integers, and $\boldsymbol{a_1}$ and $\boldsymbol{a_2}$ are the unit vectors of the hexagonal lattice.

The length of the unit vectors is defined as $a = \sqrt{3}a_{C-C}$ with the equilibrium carbon-carbon (C-C) covalent bond length a_{C-C} usually taken to be 0.1421 nm [2]. The nanotube circumference, L_c, and diameter, D_n are:

$$L_c = |\boldsymbol{C_h}| = a\sqrt{n^2 + nm + m^2} \tag{2}$$

$$D_n = \frac{L_c}{\pi} \tag{3}$$

The chiral angle, θ, is defined by the angle between the chiral vector $\boldsymbol{C_h}$ and the direction $(n, 0)$ [2] and it is given by:

$$\theta = \sin^{-1}\frac{\sqrt{3}m}{2\sqrt{n^2 + nm + m^2}} \tag{4}$$

Three major categories of carbon nanotubes can be defined based on the chiral angle θ: zigzag ($\theta = 0°$), armchair ($\theta = 30°$) and chiral ($0° < \theta < 30°$) SWCNTs. Three main symmetry groups can be also defined based on the chiral indices. In this case for armchair structure $n = m$, for zigzag structure $m = 0$, and for chiral structure $n \neq m$.

The CNT heterojunction can be represented as two CNTs that are connected by introducing an intermediate region with Stone–Wales defects [7]. Similarly to SWCNT structures, the geometrical parameters of heterojunctions (HJs) are the chirality, and diameter. There are two main heterojunction configurations [7]: (i) cone-heterojunctions (HJs of nanotubes with a given chiral angle but different radii) as armchair – armchair and zigzag – zigzag HJs, and (ii) radius-preserving heterojunctions (HJs preserving the radii, but with different chiral angles of the constituent nanotubes) as armchair – zigzag or chiral – armchair (or zigzag) HJs. According to the study of Yao *et al.* [8] most HJs (>95%) are cone-heterojunctions type.

The overall length of the heterojunction is defined as follows:

$$L_{HJ} = L_1 + L_2 + L_3 \tag{5}$$

where L_1, L_2 are the lengths of the narrower and wider SWCNTs regions, respectively, and L_3 is the length of the connecting region (see, Fig. 1).
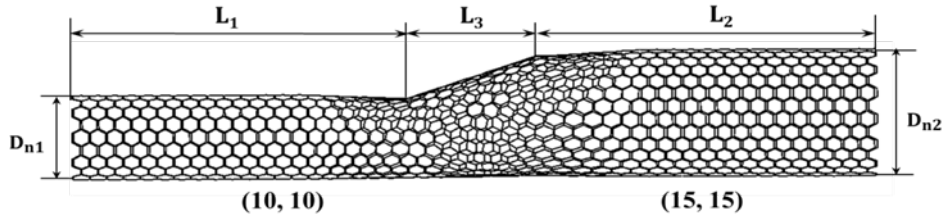
Figure 1: Geometry of cone armchair – armchair (10, 10) – (15, 15) HJ, obtained by using academic software CoNTub 1.0 © [7]

When the heterojunction consists of two SWCNTs with different diameters (i.e. cone-heterojunction), the diameter of HJ can be characterised by the average of the narrower and wider diameters (see for example: [7]):

$$\bar{D}_{HJ} = \frac{1}{2}(D_{n1} + D_{n2}) \qquad (6)$$

And the aspect ratio of the cone-heterojunction is defined as [9]:

$$\eta = \frac{L_3}{\bar{D}_{HJ}} \qquad (7)$$

The length of the connecting region, L_3, can be deduced basing on geometrical analysis [9]:

$$L_3 = \frac{\sqrt{3}}{2}\pi(D_{n2} - D_{n1}) = 2.7207(D_{n2} - D_{n1}) \qquad (8)$$

where D_{n1} and D_{n2} are diameters of the narrow and wider nanotubes, respectively.

Other relationship for the connecting region, which follows a linear function with $(D_{n2} - D_{n1})$, for armchair – armchair and zigzag – zigzag cone-heterojunctions was previously proposed [10]:

$$L_3 = 2.9157(D_{n2} - D_{n1}) \qquad (9)$$

3 NUMERICAL SIMULATION AND ANALYSIS

3.1 Finite element modelling of CNTs' structures

The NCM approach that replaces the carbon-carbon bonds of CNT by equivalent beam elements is used for modelling SWCNTs and SWCNT HJs. The finite element (FE) method uses the coordinates of the carbon atoms for generating the nodes and their suitable connection creates the beam elements. The relationships between the inter-atomic potential energies of the molecular CNT structure and strain energies of the equivalent continuum structure, consisting of beam elements undergoing axial, bending and torsional deformations, are the basis for the application of continuum mechanics to the analysis of the mechanical behaviour of SWCNTs and SWCNT HJs [5].

The meshes of the SWCNTs and SWCNT HJs structures to be used in the FE analyses, were built using the CoNTub 1.0 software [7]. This code generates ASCII files, describing atom positions and their connectivity that enter as input data in available commercial and in-

house FE codes. A previously developed in-house application, designated *InterfaceNanotubes* [6], was used to convert the ASCII files, acquired from the CoNTub 1.0 software, into the format compatible with the ABAQUS® commercial FE code. The geometrical characteristics of the SWCNTs used in the current FE analyses are summarized in Table 1. The nanotube length used in the numerical simulations was 30 times bigger than the outer diameter, so that the mechanical behaviour can be independent of the length [11].

Table 1: Geometrical characteristics of SWCNTs under study.

SWCNT type	(n, m)	D_n, nm	$\theta°$	SWCNT type	(n, m)	D_n, nm	$\theta°$
armchair	(5, 5)	0.678	30	zigzag	(14, 0)	1.096	0
	(10, 10)	1.356			(23,0)	1.802	
	(15, 15)	2.034			(32,0)	2.507	
	(20, 20)	2.713			(41,0)	3.212	
	(25, 25)	3.390			(50,0)	3.916	
	(30, 30)	4.068			(59,0)	4.618	
	(35, 35)	4.746			(77,0)	5.323	
	(40, 40)	5.424			(68,0)	6.027	
	(45, 45)	6.101			(86,0)	6.732	
	(50, 50)	6.780			(95,0)	7.436	
	(55, 55)	7.457					

The geometrical characteristics of SWCNT HJs used in the present FE analyses are summarized in Table 2. The HJs were constructed such that the lengths of the constituent nanotubes are almost equal to each other and their value is about two orders of magnitude of the length of the junction region.

Numerical simulations of conventional tensile, bending and torsion tests were carried out in order to study the mechanical properties of the SWCNTs and SWCNT HJ. In the latter case, two loading conditions, which consist of fixing the narrower and the wider side of the HJ structure, were considered.

3.2 Molecular interactions and equivalent properties of beam elements

The NCM approach uses the direct relationships between the structural mechanics parameters, i.e. tensile, $E_b A_b$, bending, $E_b I_b$, and $G_b J_b$, torsional rigidities, and the bond force field constants, k_r, k_θ, and k_τ as follows [5]:

$$\frac{E_b A_b}{l} = k_r \tag{10}$$

$$\frac{E_b I_b}{l} = k_\theta \tag{11}$$

$$\frac{G_b J_b}{l} = k_\tau \tag{12}$$

where l is the beam length equal to 0.1421 nm; E_b and G_b are the beam Young's and shear

moduli, respectively; A_b is the beam cross-sectional area; I_b and J_b are the beam moment of inertia and polar moment of inertia, respectively; and k_r, k_θ, and k_τ, are the bond stretching, bond bending and torsional resistance force constants, respectively.

Table 2: Geometrical characteristics of SWCNT HJs under study.

HJ	$(n_1, m_1) - (n_2, m_2)$	$\overline{D}_{HJ}$, nm	η	L_1, nm	L_2, nm	L_3, nm
armchair	(5, 5) – (10, 10)	1.018	1.940	100.01	99.95	1.97
armchair	(10, 10) – (15, 15)	1.696	1.166	100.06	100.00	1.98
armchair	(15, 15) – (20, 20)	2.375	0.833	100.00	100.01	1.98
zigzag	(5, 0) – (10, 0)	0.588	1.950	99.92	99.96	1.15
zigzag	(10, 0) – (15, 0)	0.979	1.177	100.14	100.12	1.15
zigzag	(15, 0) – (20, 0)	1.371	0.843	100.03	100.00	1.16

Equations 10 – 12 are the base for the application of continuum mechanics to the analysis of the mechanical behaviour of SWCNTs and SWCNT HJs. The input material and geometrical parameters of the beam element (see refs. [36, 37] from [12]) for the numerical simulations was previously summarised by the authors (see, for example [6, 10 – 12]).

4 ELASTIC PROPERTIES OF THE SINGLE-WALLED CARBON NANOTUBES

4.1 Rigidities of SWCNTs

The values of the tensile, EA, bending, EI, and torsional, GJ, rigidities were obtained from the respective numerical simulation tests results as described in the following. The tensile rigidity, EA, of SWCNT is determined as:

$$EA = \frac{F_x L}{u_x} \tag{13}$$

where F_x, is the tensile axial force applied at one nanotube end, leaving the other end fixed, L is the nanotube length and u_x is the axial displacement taken from the FE analysis.

Similarly, the bending rigidity of the nanotube, EI, is represented as:

$$EI = \frac{F_y L^3}{3u_y} \tag{14}$$

where F_y is the transverse force applied at one end of the nanotube, leaving the other fixed, u_y is the transverse displacement, taken from the FE analysis. Finally, the torsional rigidity of the nanotube, GJ, is determined as:

$$GJ = \frac{TL}{\varphi} \tag{15}$$

where T is torsional moment applied at one end of the nanotube, leaving the other fixed and φ is the twist angle, taken from the FE analysis. In case of torsion, the nodes under loading, at the end of the nanotube, are prevented from moving in the radial direction.

The evolutions of the tensile, EA, bending, EI, and torsional, GJ, rigidities with the nanotube diameter, D_n, were studied for the SWCNTs presented in Table 1. These evolutions are shown in Fig. 2. In previous studies [6, 12], the evolutions of the rigidities with nanotube diameter, D_n, were represented by a linear function for the case of the tensile rigidity, EA, and by a cubic power function for the cases of bending, EI, and torsional, GJ, rigidities, for armchair, zigzag and chiral SWCNTs, with diameters up to 2.713 nm. The fitting equations were expressed as follows, regardless of the nanotube chirality:

$$EA = \alpha(D_n - D_0) \qquad (16)$$

$$EI = \beta(D_n - D_0)^3 \qquad (17)$$

$$GJ = \gamma(D_n - D_0)^3 \qquad (18)$$

The values of the fitting parameters [6, 12] were: $\alpha = 1131.66\ nN/nm$, $\beta = 143.48\ nN/nm$, $\gamma = 130.39\ nN/nm$ and $D_0 = 3.5 \cdot 10^{-3}\ nm$.

Figure 3 shows that the current results, up to nanotube diameters equal to 7.457 nm, also follows the trends described by Eqs. 16 – 18. The values of the fitting parameters calculated based on the results of the Fig. 3 are: $\alpha = 1121.20\ nN/nm$, $\beta = 140.25\ nN/nm$ and $\gamma = 130.39\ nN/nm$, which are close to those above mentioned. Given that the value of D_0 is negligible when compared with D_n, it was discarded in the fitting of the equations (i.e. D_0 was considered equal to zero).
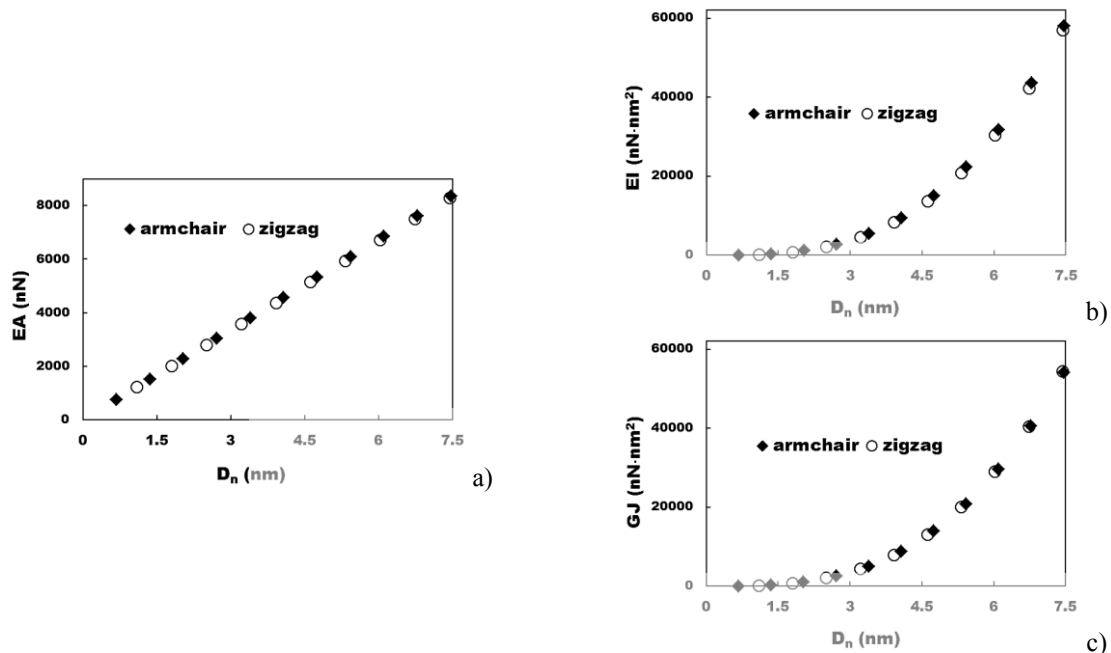

Figure 2: Evolution of: (a) the tensile, EA, (b) bending, EI, and (c) torsional, GJ, rigidities as a function of the nanotube diameter, D_n, for armchair and zigzag SWCNTs.
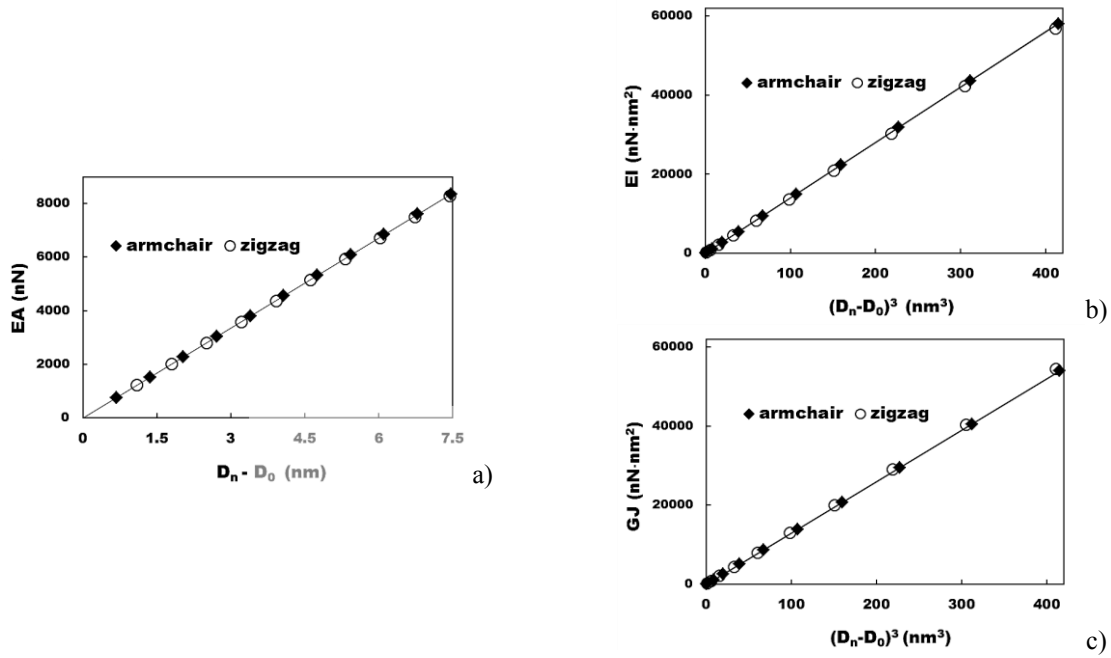
Figure 3: Evolution of: (a) the tensile, EA, rigidity as a function of $D_n - D_0$ and (b) bending, EI, and (c) torsional, GJ, rigidities, as a function of $(D_n - D_0)^3$ for armchair and zigzag SWCNTs.

The linear dependence of Eq. 16 can be understood on the base of the linear relationship between cross-sectional area and the nanotube diameter:

$$A = \frac{\pi}{4}[(D_n + t_n)^2 - (D_n - t_n)^2] = \pi D_n t_n \tag{19}$$

where t_n is the value wall thickness, which in the current study is $0.34\ nm$, equal to the interlayer spacing of graphite. In a similar way, the cubic dependences of Eqs. 17 – 18 can be understood based on the quasi-cubic relationships between the moment of inertia or the polar moment of inertia and the nanotube diameter (neglecting the value of $(t_n/D_n)^2$ in the following equations):

$$I = \frac{\pi}{64}[(D_n + t_n)^4 - (D_n - t_n)^4] = \frac{\pi D_n^3 t_n}{8}\left[1 + \left(\frac{t_n}{D_n}\right)^2\right] \tag{20}$$

$$J = \frac{\pi}{32}[(D_n + t_n)^4 - (D_n - t_n)^4] = \frac{\pi D_n^3 t_n}{4}\left[1 + \left(\frac{t_n}{D_n}\right)^2\right] \tag{21}$$

4.2 Young's and shear moduli of SWCNTs

The Young's modulus of the SWCNT is calculated, taking into account the tensile, EA, and bending, EI, rigidities, using the following expression [6]:

$$E = \frac{EA}{A} = \frac{EA}{\pi t_n \sqrt{8\left(\frac{EI}{EA}\right) - t_n^2}} \tag{22}$$

The shear modulus of the SWCNT is calculated, taking into account the tensile, EA, bending, EI, and torsional, GJ, rigidities by following equation [12]:

$$G = \frac{GJ}{J} = \frac{GJ}{2\pi t_n \left(\frac{EI}{EA}\right)\sqrt{8\left(\frac{EI}{EA}\right) - t_n^2}} \tag{23}$$

The relationships 16 – 18 and the knowledge of the values of the parameters α, β, γ allow the easy evaluation of the Young's and the shear moduli as a function of the nanotube diameter, without resorting to the numerical tests (D_0 was neglected in these equations):

$$E = \frac{\alpha D_n}{\pi t_n \sqrt{8\frac{\beta}{\alpha}D_n^2 - t_n^2}} \tag{24}$$

$$G = \frac{\gamma D_n}{2\pi t_n \left(\frac{\beta}{\alpha}\right)\sqrt{8\frac{\beta}{\alpha}D_n^2 - t_n^2}} \tag{25}$$

In the Fig. 4 (a, b) the values of the Young's modulus and shear modulus calculated by Eqs. 22 and 23, are plotted as a function of the nanotube diameter, D_n. The evolutions of the Young's modulus and shear modulus, obtained by Eqs. 24 and 25, are also shown in Fig. 4. The Young's modulus of SWCNTs decreases with increase of the nanotube diameter, and with further increase of the nanotube diameter, the Young's modulus tends to an approximately constant value as it is shown in the Fig. 4a. The same trend is observed for the evolution of the shear modulus with D_n (see, Fig. 4b). These trends in the evolution of the Young's and shear moduli with nanotube diameter extend up to diameters of about 7.5 nm, the trends already described for SWCNTs with diameters up to about 2.7 nm [6, 12]. Eqs. 24 and 25 allow obtaining acurate evolutions of the Young's and shear moduli, respectively, without resorting to the numerical simulation.
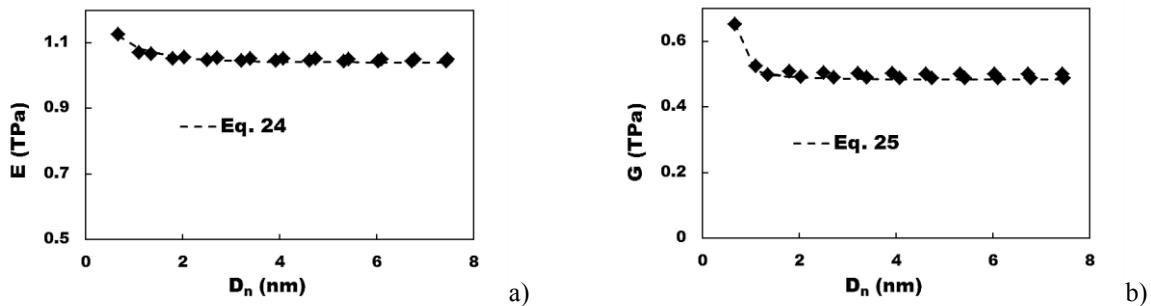

Figure 4: Evolution of: (a) Young's modulus, E, and (b) shear modulus, G, of SWCNTs as a function of the nanotube diameter, D_n.

5   ELASTIC PROPERTIES OF THE SINGLE-WALLED CARBON NANOTUBES HETEROJUNCTIONS

5.1 Rigidities of SWCNT HJs

The analysis of the mechanical behaviour of the armchair – armchair and zigzag – zigzag HJs, pointed out the occurrence of redundant bending deformation during the tensile test, making it difficult to analyse this test [10]. Therefore, we analyse the mechanical behaviour under bending and torsion.

The bending rigidity, $(EI)_{HJ}$, is obtained from the respective numerical simulation tests results as follows:

$$(EI)_{HJ} = \frac{F_y L_{HJ}{}^3}{3u_y} \tag{26}$$

where L_{HJ} is the heterojunction length, F_y is the transverse force applied at one end of the nanotube, leaving the other fixed, u_y is the transverse displacement, taken from the FE analysis. The torsional rigidity, $(GJ)_{HJ}$, is determined by:

$$(GJ)_{HJ} = \frac{T L_{HJ}}{\varphi} \tag{27}$$

where T is torsional moment applied at one end of the nanotube, leaving the other fixed and φ is the twist angle, taken from the FE analysis. The nodes under loading, at the end of the nanotube, are prevented from moving in the radial direction.

The $(EI)_{HJ}$ and $(GJ)_{HJ}$ rigidities for armchair-armchair and zigzag-zigzag HJs were plotted in Fig. 5 as a function of the heterojunction aspect ratio, $\eta = L_3/\overline{D}_{HJ}$ (see Fig. 1). Both rigidities, $(EI)_{HJ}$ and $(GJ)_{HJ}$ for armchair-armchair and zigzag-zigzag HJs increase with the increasing of the η. The bending and torsional rigidities for armchair-armchair HJs are higher than those for zigzag-zigzag HJs. The difference between the $(EI)_{HJ}$ values for armchair – armchair HJs and zigzag – zigzag HJs is more significant when the force is applied to the narrower nanotube. On the contrary, the evolution of the torsional rigidity with the aspect ratio, η is not sensitive to the loading condition: the $(GJ)_{HJ}$ values are at about the same whether the torsional moment is applied to the wider or narrower nanotube.

The bending, $(EI)_{HJ}$, and torsional, $(GJ)_{HJ}$, rigidities of the HJ structures can be calculated knowing the rigidities of the constituent SWCNTs. In fact, using Eq. 26 (or more suitably the equation of beam deflection) and Eq. 27, it is possible to obtain both rigidities for the HJs structures, considering that the respective transverse displacement (bending test) or the twist angle (torsion test) are equal to the sums of the corresponding transverse displacements or twist angles of each SWCNT constituent of the HJs:

$$(EI)_{HJ} = \frac{L_{HJ}^3}{\left(\dfrac{L_a^3}{(EI)_a} + \dfrac{3L_a^2 L_f + 3L_a L_f^2 + L_f^3}{(EI)_f} \right)} \tag{28}$$

$$(GJ)_{HJ} = \frac{L_{HJ}}{\left(\dfrac{L_a}{(GJ)_a} + \dfrac{L_f}{(GJ)_f}\right)} \qquad (29)$$

where L_{HJ} is the overall length of HJ; $(EI)_a$ and $(EI)_f$ are the bending rigidities of the constituent SWCNTs and $(GJ)_a$ and $(GJ)_f$ are their torsional rigidities; L_a and L_f are the lengths of the constituent SWCNTs; the letters a and f refer to the nanotubes to which the force is applied and is fixed, respectively.
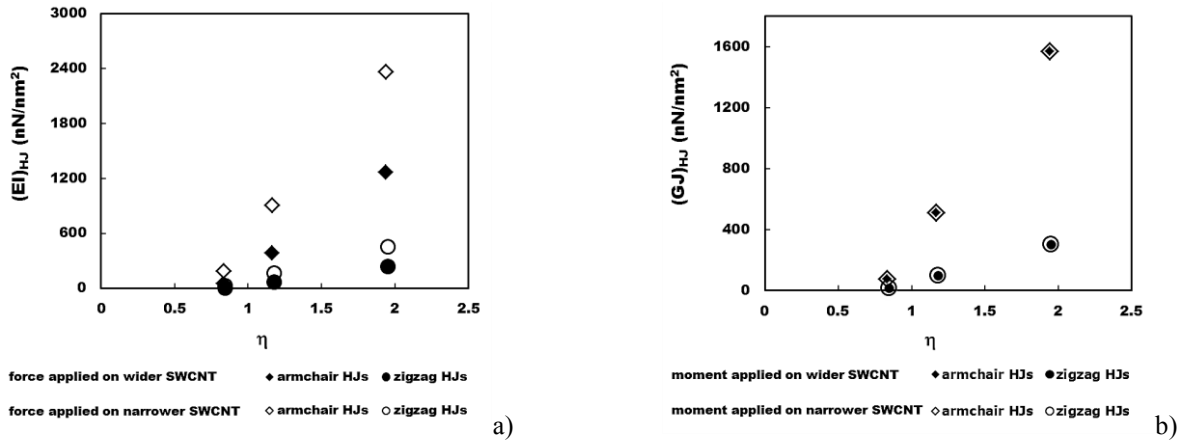

Figure 5: Evolution of: (a) $(EI)_{HJ}$ rigidity and (b) $(GJ)_{HJ}$ rigidity with the heterojunction aspect ratio, η, for armchair – armchair and zigzag – zigzag HJs.

Figure 6 compares the values of the rigidities ($(EI)_{HJ}$ – Fig. 6a; $(GJ)_{HJ}$ – Fig. 6b) obtained from FE analysis (Eqs. 26 and 27) and those calculated with help of Eqs. 28 and 29. The results of the Fig. 6 evidence the accuracy of the proposed analytical solutions for evaluation of the bending and torsional rigidities of armchair – armchair and zigzag – zigzag heterojunctions. The mean difference between the values of rigidities, evaluated by Eqs. 28 and 29 and those obtained from FE analysis, is 1.22% for the $(EI)_{HJ}$ rigidity and 1.74% for the $(GJ)_{HJ}$ rigidity.
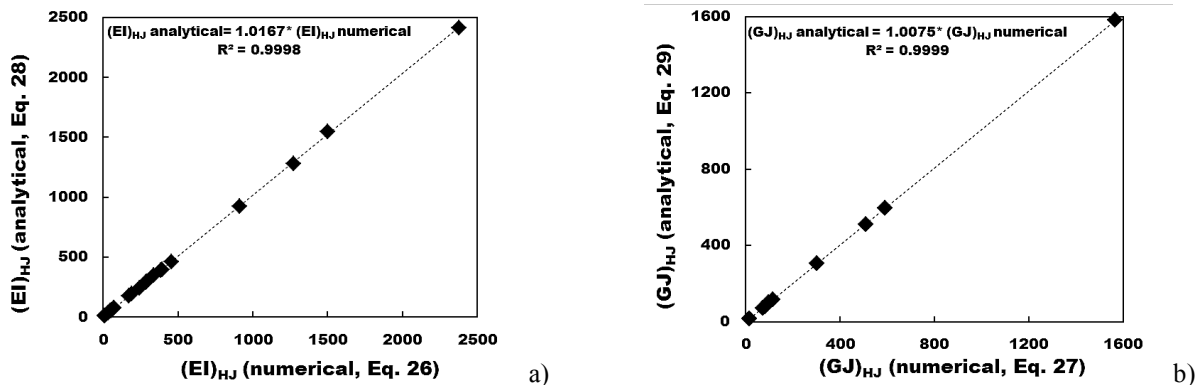

Figure 6: Comparison of: (a) bending, $(EI)_{HJ}$ and (b) torsional, $(GJ)_{HJ}$ rigidities obtained from FE analysis and evaluated by Eqs. 28 and 29, for armchair – armchair and zigzag – zigzag HJs.

5.2 Young's and shear moduli of SWCNT HJs

The bending and torsional rigidities obtained from FE analysis were used for the evaluation of the heterojunction Young's, E_{HJ}, and shear, G_{HJ}, moduli equivalent to a SWCNT with diameter given by $\bar{D}_{HJ} = \frac{1}{2}(D_{n1} + D_{n2})$, respectively:

$$E_{HJ} = \frac{(EI)_{HJ}}{I_{HJ}} = \frac{(EI)_{HJ}}{\frac{\pi}{64}\left[\left(\bar{D}_{HJ} + t_n\right)^4 - \left(\bar{D}_{HJ} - t_n\right)^4\right]} \tag{30}$$

$$G_{HJ} = \frac{(GJ)_{HJ}}{J_{HJ}} = \frac{(GJ)_{HJ}}{\frac{\pi}{32}\left[\left(\bar{D}_{HJ} + t_n\right)^4 - \left(\bar{D}_{HJ} - t_n\right)^4\right]} \tag{31}$$

where $t_n = 0.34\ nm$ is the value of the nanotube wall thickness.

The Young's modulus and shear modulus of armchair-armchair and zigzag-zigzag SWCNT HJs were plotted as a function of the heterojunction aspect ratio, η (Fig. 7). Both, Young's modulus and shear modulus decrease with increasing of the HJ aspect ratio. Also, the Young's modulus of HJs is sensitive to the loading condition: the value of E_{HJ} is higher when the force is applied on the narrower nanotube. The difference between the E_{HJ} values of armchair – armchair HJs and zigzag – zigzag HJs is less significant when the force is applied on the narrower nanotube. On the contrary, shear modulus of HJs is insensitive to the loading condition: the value of G_{HJ} does not change when the torsional moment is applied on the wider or narrower nanotube. The difference observed between shear modulus of armchair HJs and zigzag HJ is relatively small.
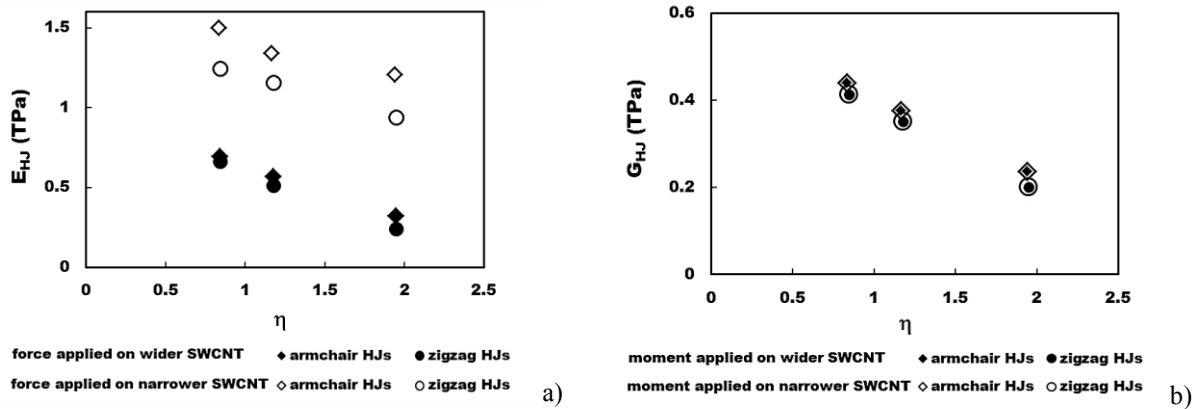

Figure 7: Evolution of the Young's modulus (a) and shear modulus (b) with the heterojunction aspect ratio for armchair – armchair and zigzag – zigzag HJs.

6   CONCLUSIONS

- Equations 16 – 18 establishing relationships between each of three rigidities and the nanotube diameter allowing the easy evaluation of the Young's modulus and shear modulus of SWCNTs by using Equations 24 and 25, without resorting to numerical simulation;
- Equations 28 and 29 allow the easy evaluation of the bending and torsion rigidities of

HJs structures, from the respective rigidities of the constituents SWCNT. These allows the accurate evaluation of the Young's and shear moduli of the SWCNTs, equivalent to the HJs structures.

ACKNOLEDGEMENTS

REFERENCES

[1] Robertson, J. Realistic applications of CNTs. *Mater Today* (2004) **7**: 46-52.

[2] Dresselhaus, M.S., Dresselhaus, G., Avouris, Ph. *Carbon Nanotubes: Synthesis, Structure, Properties, and Applications*, Springer Book Series: Topics in Applied Physics, Springer-Verlag Berlin Heidelberg, Germany, 80, (2001).

[3] Wei, D.C. and Liu, Y.Q. The intramolecular junctions of carbon nanotubes. *Adv Mater* (2008) **20**: 2815-2841.

[4] Wang, L., Zhang, Z., Han, X. In situ experimental mechanics of nanomaterials at the atomic scale. *NPG Asia Mater* (2013) **5**: e40-11.

[5] Li, C. and Chou, T.W. A structural mechanics approach for the analysis of carbon nanotubes. *Int J Solids Struct* (2003) **40**: 2487-2499.

[6] Sakharova, N.A., Pereira, A.F.G., Antunes, J.M., Brett, C.M.A., Fernandes, J.V. Mechanical characterization of single-walled carbon nanotubes: Numerical simulation study. *Compos Part B-Eng.* (2015) **75**: 73-85.

[7] Melchor, S. and Dobado, J.A. CoNTub: An algorithm for connecting two arbitrary carbon nanotubes. *J Chem Inf Comp Sci* (2004) **44**: 1639-1646.

[8] Yao, Y.G., Li, Q.W., Zhang, J., Liu, R., Jiao, L.Y., Zhu, Y.T., Liu, Z.F. Temperature-mediated growth of single-walled carbon-nanotube intramolecular junctions. *Nat Mater* (2007) **6**: 283-286.

[9] Qin, Z., Qin, Q.-H., Feng, X.-Q. Mechanical property of carbon nanotubes with intramolecular junctions: Molecular dynamics simulations. *Phys Lett A* (2008) **372**: 6661-6666.

[10] Sakharova, N.A., Pereira, A.F.G., Antunes, J.M., Fernandes, J.V. Numerical simulation of the mechanical behaviour of single-walled carbon nanotubes heterojunctions. *J Nano Res* (2016) **38**: 73- 87.

[11] Sakharova, N.A., Pereira, A.F.G., Antunes, J.M., Fernandes, J.V. Numerical simulation on the mechanical behaviour of the multi-walled carbon nanotubes. *J Nano Res* (2017) **47**: 106-119.

[12] Pereira, A.F.G., Antunes, J.M., Fernandes, J.V., Sakharova, N.A. Shear modulus and Poisson's ratio of single-walled carbon nanotubes: numerical evaluation. *Phys Status Solidi B* (2016) **253**: 366-376.